POLITECNICO DI TORINO
Repository ISTITUZIONALE

Finite elements based on Jacobi shape functions for the free vibration analysis of beams, plates, and shells

Original
Finite elements based on Jacobi shape functions for the free vibration analysis of beams, plates, and shells / Carrera, E., Scano, D.. - In: MECHANICS OF ADVANCED MATERIALS AND STRUCTURES. - ISSN 1537-6532. - (2024), pp. 1-9. [10.1080/15376494.2023.2219438]

Availability:
This version is available at: 11583/2982524 since: 2023-09-27T13:18:20Z

Publisher:
Taylor & Francis

Published
DOI:10.1080/15376494.2023.2219438

Terms of use:

This article is made available under terms and conditions as specified in the corresponding bibliographic description in the repository

Publisher copyright
Taylor and Francis postprint/Author's Accepted Manuscript con licenza CC by-nc

This is an Accepted Manuscript version of the following article: Finite elements based on Jacobi shape functions for the free vibration analysis of beams, plates, and shells / Carrera, E., Scano, D.. - In: MECHANICS OF ADVANCED MATERIALS AND STRUCTURES. - ISSN 1537-6532. - (2024), pp. 1-9. [10.1080/15376494.2023.2219438]. It is deposited under the terms of the CC BY- NC License

(Article begins on next page)

27 November 2026

Finite elements based on Jacobi shape functions for the free vibration analysis of beams, plates, and shells

Erasmo Carrera[1,a,b], Daniele Scano[2,a]

[a]Mul2 Lab, Department of Mechanical and Aerospace Engineering, Politecnico di Torino, Corso Duca degli Abruzzi 24, 10129 Torino, Italy.

[b]Department of Mechanical Engineering, College of Engineering, Prince Mohammad Bin Fahd University, P.O. Box 1664, Al Khobar 31952, Kingdom of Saudi Arabia

Keywords: Finite element method; beam, plate, and shell models; Jacobi polynomials; shear locking; free vibration analysis; Carrera unified formulation.

Abstract. This paper proposes the use of Jacobi polynomials as shape functions for the free vibration analysis of beam, plate, and shell structures. Jacobi polynomials, indicated as $P_p^{(\gamma,\theta)}$, belong to the family of classical orthogonal polynomials, and depend on two scalar parameters γ and θ, with p being the polynomial order. The Jacobi-like shape functions are built in the context of the Carrera unified formulation, which permits the expression of displacement kinematics in a hierarchical form. In this manner, it is possible to adopt several classical to complex higher-order theories with ease. Particular attention is focused on the attenuation and the correction of the shear locking. The results have been compared with analytical results from the literature. For the plate benchmark, analytical results are introduced as the reference results in this paper for the first time using the closed form of CUF. Beams, plates, and shells with different thicknesses have been considered. It is demonstrated that the parameters γ and θ are not influential for the calculations.

1 Introduction

Modern engineering has required complicated and computationally expensive structural analyses. In particular, the free vibration analysis is a crucial point at the beginning of the design process. However, for some geometries and to reduce the computer power, appropriate 1D and 2D models can be adopted. The Finite Element Method (FEM) is undoubtedly the most used computational technique for structural analysis, see McNeal [1].

The majority of Finite Element (FE) formulations use axiomatic-type theories. Considering the beam theories, Euler-Bernoulli Beam Model (EBBM) [2] and Timoshenko Beam Model (TBM) [3] are the classical formulations and are still adopted in practical problems. For both, the cross-section is assumed to be rigid in its plane. For EBBM, the shear deformation is neglected, while it is considered constant along the cross-section in the case of TBM. More refined FEs were implemented. See Carrera et al. [4]. In either classical or high-order beam models, Lagrange -like shape functions are mainly used to build one-dimensional (1D) FEs. Eventually, two-, three- and four-node 1D FEs have been developed, see Bathe [5]. Carrera et al. [6] used the same elements in the framework of Carrera Unified Formulation (CUF) for static and vibrational problems.

As far as two-dimensional (2D) plate and shell FEs are considered, Thin Plate Theory (TPT) and Thin Shell Theory (TST) represent the classical models. TPT and TST are based on Kirchhoff [7] hypotheses which impose that the line remains orthogonal to the plate/shell reference surface during deformation. When the transverse shear deformation is added, the Reissner–Mindlin [8,9]

[1] Full Professor. E-mail: erasmo.carrera@polito.it

[2] PhD Student. Corresponding author. E-mail: daniele.scano@polito.it

theory (also known as First-Order Shear Deformation Theory, FSDT) can be built. Considering the shell, TST is an example of the Love first approximation theory, while FSDT is a Love second approximation theory. The classical ones were the most used structural theories, even though they do not satisfy the compatibility requirements, see Argyris [10]. The majority of plate/shell elements are based on Lagrange polynomials. Bathe and Ho [11] reviewed several quadrilateral Lagrange-based elements: four-, eight-, nine- and sixteen-node isoparametric shell elements. Furthermore, Carrera [12] used four-, eight- and nine-node FEs to study composite plates.

In the present paper, Jacobi polynomials are utilized for building shape functions in the free vibration analysis of beams, plates, and shells in CUF. Carrera et al. [13] first used these polynomials to build structural theories for beams (for the cross-section), plates, and shells (along the thickness) in the framework of CUF. The analysis was centered on static cases. Jacobi polynomials are classical orthogonal polynomials, and they can be derived from a recurrence relation. They can originate a vast class of polynomials by changing the two parameters γ and θ, i.e., Legendre, Chebyshev, see the book of Abramowitz and Stegun [14]. Concerning the shape functions, Fuentes et al. [15] proposed FEs based on shifted integrated Jacobi polynomials, considering the parameter θ null. Several shapes are introduced for 1D, 2D, and three-dimensional (3D) elements. Szabo et al. [16] proposed a hp-version of FE derived from Legendre polynomials for beam, plate, and solid. In this method, it is possible to increase both the number of elements and the polynomial order of the shape function. Adopting general Jacobi polynomials, the Legendre case can be derived with γ and θ equal to zero. Zappino et al. [17] compared Legendre and Lagrange shape functions for 2D plate elements in the static analysis of multilayered structures. The p-version shape functions can alleviate the locking by increasing the polynomial order without using other interpolation functions and extra loops as in the MITC method. See Cinefra [18] for the use of this method in the CUF framework. Concerning the expansion functions in CUF, Pagani et al. [19] used Legendre polynomials for 2D cross-section in beam formulation, while Cinefra and Valvano [20] studied plates by means of hierarchical 1D expansions built from Legendre polynomials.

In this paper, several structural expansions are considered, from the classical models to the Higher-Order Theories (HOT) derived from the Taylor polynomials. The CUF is versatile since the governing equations are invariant from the adopted structure theory. For example, in the domain of CUF theories, Pagani et al. [21] used HOT for free vibration analysis of thin-walled beams, while Carrera [22] proposed general HOT for the analysis of plates and shells.

The present work deals with the free vibration analysis of beams, plates, and shells. Several contributions have been proposed during the last few years. Kapania and Raciti [23] reviewed the recent developments in the vibrations of beams and plates. Carrera et al. [24] used polynomial, trigonometric, exponential, and zig-zag theories for the free vibrations of laminated beams. Yan et al. [25] studied curved metallic and composite beams with Legendre-like structural theories. Carrera [22] extended the use of refined theories to plates and shells. For instance, Cinefra and Soave [26] analyzed multilayered plates made of functionally graded materials with Taylor and Lagrange expansions through the thickness. Concerning the free vibration analysis of shells, Soldatos [27] presented a survey and illustrated numerical results for Donnell [28], Love, Sanders [29], and Flügge [30] theories. Loy et al. [31] studied isotropic and functionally graded shells for free vibration analysis by using the Love shell theory. Matsunaga [32] included the effects of higher-order deformations and rotatory inertia for aminated circular cylindrical shells. Carrera [33] deeply investigated the TST and FSDT in Donnell, Love, and Flügge theories. Finally, Zappino et al. [34] studied reinforced thin-walled structures with longitudinal stiffeners by using 1D and 2D shell elements in the same models. Both Taylor and Lagrange polynomials were used.

This paper is structured as follows: Section 2, *Shape functions based on Jacobi polynomials*, briefly introduces this new kind of shape functions for 1D and 2D elements. Section 3, *Formulation of finite elements*, gives background information about the CUF framework for beams, plates, and shells. Section 4, *Governing equations and Finite Element matrices*, briefly illustrates the passages to build the matrices in the CUF for a free vibration analysis. Section 5, *Results*, presents interesting comparisons by adopting classical and refined theories for both thick and thin structures. Finally, the most relevant conclusions of this work are drawn.

2 Shape functions based on Jacobi polynomials

This paper exploits the Jacobi polynomials to build shape functions for beams, plates, and shells. These elements have the excellent capability to use hierarchical features. In this way, one can automatically build advanced shape functions by simply choosing the polynomial order *p*, while keeping the mesh fixed. At the same time, it is also possible to increment the number of FEs. Jacobi polynomials are formulated using recurrence relations. See the book of Abramowitz and Stegun [14]. The formula used to describe the orthogonal Jacobi polynomials is:

$$P_p^{(\gamma,\theta)}(\zeta) = \left(A_p + B_p\right)P_{p-1}^{(\gamma,\theta)}(\zeta) - C_p P_{p-2}^{(\gamma,\theta)}(\zeta) \tag{1}$$

where γ and θ are two scalar parameters and p is the order of the polynomial. The formula is calculated in natural plane $\zeta = [-1, +1]$. The first values are $P_0^{(\gamma,\theta)}(\zeta) = 1$ and $P_1^{(\gamma,\theta)}(\zeta) = A_0\zeta + B_0$. The parameters A_p, B_p, and C_p can be found in [14]. By choosing γ and θ, other popular polynomials can be devised.

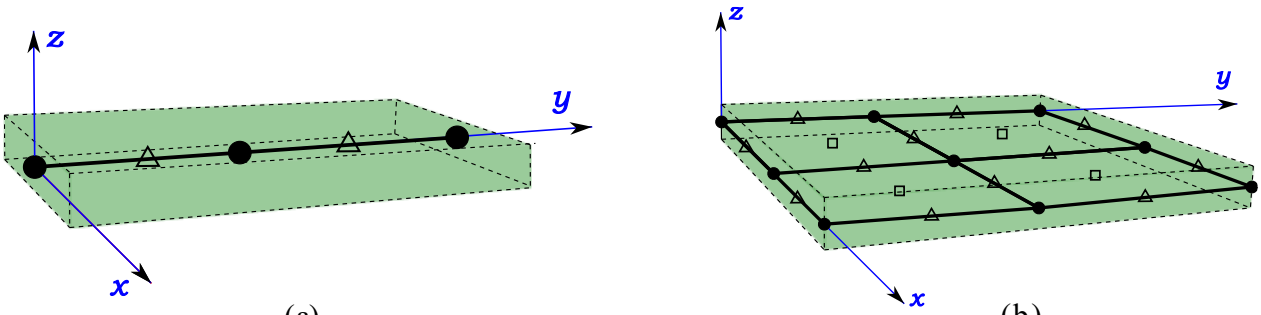

(a) (b)

Figure 1: Beam (a), and plate/shell (b) elements for Jacobi shape functions. Definition of nodes ●, edges △, and faces □.

2.1 Application to beams

In this case, two types of polynomials are used along the y-axis: vertex (or node) and edge. Szabo et al. [16] proposed a procedure to build these types of FEs. As a matter of fact, there are two vertexes and a number of edge modes that depend on the polynomial order of the chosen elements. For instance, Fig. 1 (a) illustrates the FEM discretization for a beam.
The hierarchic functions are defined as:

$$\begin{aligned} N_1(\zeta) &= \frac{1}{2}(1-\zeta) \\ N_2(\zeta) &= \frac{1}{2}(1+\zeta) \\ N_i(\zeta) &= \phi_{i-1}(\zeta), \;\; i = 3,4,\dots,p+1 \end{aligned} \tag{2}$$

with

$$\phi_j(\zeta) = (1-\zeta)(1+\zeta)P_{j-2}^{(\gamma,\theta)}(\zeta), \quad j = 2,3,\dots,p \tag{3}$$

where p indicates the polynomial order. Given the following property

$$N_i(-1) = N_i(1) = 0, \ i \geq 3 \tag{4}$$

the functions $N_i(\zeta), i = 3,4,...$ are named bubble functions or edge expansions. On the other hand, the first two functions N_1 and N_2 are the vertex expansions.

2.2 Application to plates and shells

Figure 1 (b) depicts the FEM discretization for a plate structure. In this shape function, three kinds of polynomials are used over the $x-y$ plane: vertex, edge, and internal. There are four vertex modes that vanish at all nodes but one. Contrarily, the number of edge modes changes according to the polynomial order of the FE, and they vanish for all sides of the domain but one. Finally, the internal modes are included from the fourth-order polynomial. They dissapear at all sides. See [20] for more information. The vertex modes are written as follows:

$$N_i(\xi,\eta) = \tfrac{1}{4}(1-\xi_i\xi)(1-\eta_i\eta), \ i = 1,2,3,4 \tag{5}$$

where ξ and η are calculated in the natural plane between -1 and +1, and ξ_i and η_i are the vertexes. From $p \geq 2$, the edge modes arise in the natural plane as follows

$$\begin{aligned} N_i &= \tfrac{1}{2}(1-\eta)\phi_p(\xi), i = 5,9,13,18,\dots \\ N_i &= \tfrac{1}{2}(1+\xi)\phi_p(\eta), i = 6,10,14,19,\dots \\ N_i &= \tfrac{1}{2}(1+\eta)\phi_p(\xi), i = 7,11,15,20,\dots \\ N_i &= \tfrac{1}{2}(1-\xi)\phi_p(\eta), i = 8,12,16,21,\dots \end{aligned} \tag{6}$$

where p represents the polynomial degree of the bubble function $\phi_j(\zeta)$. Internal expansions are inserted for $p \geq 4$, they vanish at all the edges of the quadrilateral domain. There are $(p-2)(p-3)/2$ internal polynomials. By multiplying 1D edge modes, N_i internal expansions are built. For instance, considering the fifth-order polynomials, three internal expansions are found, which are

$$\begin{aligned} N_{17}(\xi,\eta) &= \phi_2(\xi)\phi_2(\eta), \ 2+2=4 \\ N_{22}(\xi,\eta) &= \phi_3(\xi)\phi_2(\eta), \ 3+2=5 \\ N_{23}(\xi,\eta) &= \phi_2(\xi)\phi_3(\eta), \ 2+3=5 \end{aligned} \tag{7}$$

3 Formulation of finite elements

Figure 2 shows beam, plate, and shell structures.

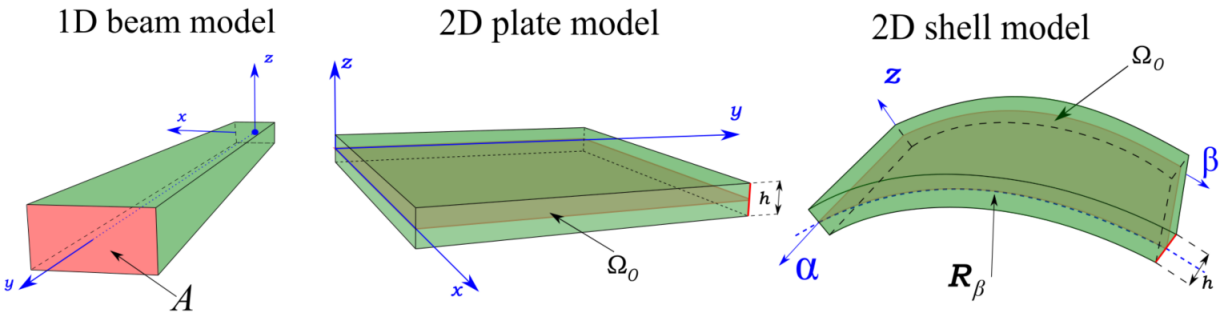

Figure 2: Generic beam, plate, and shell structures. The 1D beam and 2D plate models (x, y, z) employ a Cartesian reference system. The 2D shell model adopts a curvilinear reference system (α, β, z).

1D and 2D plate models adopt a Cartesian reference system. The cross-section A of the beam lays on the $x-z$ plane. Thence, the beam axis is placed along the y direction. On the other hand, the 2D plate model uses the z coordinate for the thickness direction, and the coordinates x and y indicate the in-plane mid-surface Ω_0. Finally, a curvilinear reference frame (α, β, z) is adopted in a shell model to account for the curvature. The three-dimensional displacement fields are the followings:

$$\mathbf{u}(x,y,z) = \{u_x, u_y, u_z\}^T, \ \mathbf{u}(\alpha,\beta,z) = \{u_\alpha, u_\beta, u_z\}^T \tag{8}$$

In this paper, the Carrera Unified Formulation (CUF) is adopted to describe the 3D displacement field compactly. Furthermore, a generic expansion of the primary mechanical variables through the use of arbitrary functions of the domain is written as follows:

$$\mathbf{u}(x,y,z) = F_\tau \mathbf{u}_\tau, \quad u(\alpha,\beta,z) = F_\tau \mathbf{u}_\tau, \quad \tau = 1,2,\dots,M \tag{9}$$

where F_τ are the expansion functions of the generalized displacements $\mathbf{u}_\tau$, while τ denotes summation and M is the order of expansion. The independent variables are explicitly shown for each formulation in Table 1.

Table 1: CUF Formulation. τ denotes summation with τ = 1, …, M while M is the order of expansion.

Formulation	3D Fields	CUF Expansions	
1D BEAM	$\mathbf{u}(x,y,x)$	$F_\tau(x,z)$	$\mathbf{u}_\tau(y)$
2D PLATE	$\mathbf{u}(x,y,x)$	$F_\tau(z)$	$\mathbf{u}_\tau(x,y)$
2D SHELL	$\mathbf{u}(\alpha,\beta,x)$	$F_\tau(z)$	$\mathbf{u}_\tau(\alpha,\beta)$

In the framework of CUF, a generic structural theory can be freely adopted. In particular, Taylor - like polynomials can be used to build several classical and refined theories. Concerning the beam formulation, Taylor expansion uses 2D polynomials $x^i z^j$ as base, where i and j are positive integers. Pagani et al. [20] used Taylor expansions in the CUF for beams to account for non-classical effects. When plates and shells are considered, Taylor expansion adopts 1D polynomials z^j as the base. Carrera [35] used several refined theories, e.g., a third-order theory. Then, classical theories can be derived as degenerated cases from the first-order Taylor expansion. See [6] for a detailed explanation. The Taylor structural theories are indicated as TP, where P is the polynomial order.

The CUF and the Finite Element Method (FEM) are adopted together to provide numerical results. FEM discretizes the generalized displacements $\mathbf{u}_{\boldsymbol{\tau}}$. If the equations in Table 1 are recalled, generalized displacements are approximated as illustrated in Table 2. N_i indicates the shape functions, where the repeated subscript i indicates summation. N is the number of the shape functions per element. Finally, $\mathbf{q}_{\boldsymbol{\tau i}}$ are the following vectors of the FE nodal parameters:

$$\mathbf{q}_{\tau i}(x,y,z) = \left\{q_{x_{\tau i}}, q_{y_{\tau i}}, q_{z_{\tau i}}\right\}^T, \ \mathbf{q}_{\tau i}(\alpha,\beta,z) = \left\{q_{\alpha_{\tau i}}, q_{\beta_{\tau i}}, q_{z_{\tau i}}\right\}^T \tag{10}$$

Table 2: Introduction of FE discretization. i is the repeated index with i=1, …, N where N is the number of shape functions per element.

Formulation	3D Fields	FEM and CUF Expansion		
1D BEAM	$\mathbf{u}(x,y,z)$	$N_i(y)$	$F_\tau(x,z)$	$\mathbf{q}_{\tau i}$
2D PLATE	$\mathbf{u}(x,y,z)$	$N_i(x,y)$	$F_\tau(z)$	$\mathbf{q}_{\tau i}$
2D SHELL	$\mathbf{u}(\alpha,\beta,z)$	$N_i(\alpha,\beta)$	$F_\tau(z)$	$\mathbf{q}_{\tau i}$

In this work, novel Jacobi FEs are used. These shape functions are denoted to as J*P*, where *P* is the polynomial order. In particular, J1, J2, J3, J4, and J5 are used for both beams and 2D plates and shells.

4 Governing equations and Finite Element matrices

As usual, it is useful to express stress, $\boldsymbol{\sigma}$, and strain, $\boldsymbol{\epsilon}$, tensors in vectorial form as follows:

$$\begin{aligned} \boldsymbol{\sigma} &= \{\sigma_{xx} \quad \sigma_{yy} \quad \sigma_{zz} \quad \sigma_{xz} \quad \sigma_{yz} \quad \sigma_{xy}\}^T \quad \boldsymbol{\epsilon} = \{\epsilon_{xx} \quad \epsilon_{yy} \quad \epsilon_{zz} \quad \epsilon_{xz} \quad \epsilon_{yz} \quad \epsilon_{xy}\}^T \\ \boldsymbol{\sigma} &= \{\sigma_{\alpha\alpha} \quad \sigma_{\beta\beta} \quad \sigma_{zz} \quad \sigma_{\alpha z} \quad \sigma_{\beta z} \quad \sigma_{\alpha\beta}\}^T \quad \boldsymbol{\epsilon} = \{\epsilon_{\alpha\alpha} \quad \epsilon_{\beta\beta} \quad \epsilon_{zz} \quad \epsilon_{\alpha z} \quad \epsilon_{\beta z} \quad \epsilon_{\alpha\beta}\}^T \end{aligned} \tag{11}$$

The geometrical relations between strains and displacements are defined as:

$$\boldsymbol{\epsilon} = \mathbf{b}\mathbf{u} \tag{12}$$

where $\mathbf{b}$ is the matrix of differential operators in the case of small displacements and angles of rotations. See Carrera et al. [6,20] for more details. Furthermore, linear elastic isotropic materials are considered. The constitutive relation can be written as follows:

$$\boldsymbol{\sigma} = \mathbf{C}\boldsymbol{\epsilon} \tag{13}$$

where $\mathbf{C}$ is the material elastic matrix, see [5] for the explicit form.

The principle of virtual displacements is used to derive the governing equations:

$$\int_V \delta\boldsymbol{\epsilon}^{\boldsymbol{T}}\boldsymbol{\sigma}\, dV = -\int_V \delta\mathbf{u}\rho\ddot{\mathbf{u}} dV \tag{14}$$

where V is the volume integration domain, ρ is the density of the material and $\ddot{\mathbf{u}}$ is the acceleration vector. The left-hand side of the equation represents the variation of the internal work, while the virtual variation of the work performed by inertial loads is represented by the right-hand side. Recalling the constitutive equations Eq. (13), the geometrical Eq. (12), FEM and CUF relations from the Table 2, the following governing equations can be written:

$$\delta\mathbf{q}_{sj}^T : \mathbf{K}^{ij\tau s}\, \mathbf{q}_{\tau i}^T = -\mathbf{M}^{ij\tau s}\ddot{\mathbf{q}}_{\tau i} \tag{15}$$

$\mathbf{K}^{ij\tau s}$ and $\mathbf{M}^{ij\tau s}$ are 3×3 matrices, which are named as fundamental nucleus of the stiffness and mass matrices, respectively. The explicit relations of the components are given in [6]. After the general assembly and the introduction of the harmonic solution, the following eigenvalue problem is written:

$$(-\omega_n^2 \mathbf{M} + \mathbf{K})\mathbf{U}_n = \mathbf{0} \tag{16}$$

where $\mathbf{U}_n$ is the *n*th eigenvector.

5 Results

In this section, three study cases are shown. The numerical examples are compared to analytic solutions from the literature when they are available. Several Jacobi-like shape functions are implemented. Concerning structural theories, both classical and higher-order models are employed. Convergence analyses are performed to understand the numerical properties of the introduced shape functions. The results are normalized respect to the reference solutions. Similar degrees of Freedom (DOF) are used to compare different Jacobi theories. In this way, a different Number of FEs (N^o FEs) is adopted for each model. Finally, the analysis of the influence of γ and θ has not been explicitly shown in the paper for the sake of brevity, given that γ and θ are not influential.

5.1 Isotropic beam

The first analysis case presented is a beam. The geometric characteristics are described in Fig. 3. The cross-section is a solid square with $b = h = 0.2$ [m]. The material properties are $E = 75$ [GPa], $\nu = 0.33$ and the material density, $\rho = 2700$ [kg/m^3]. The study case is taken from [36]. Present results are compared with closed form solutions. Two analyses are performed. In the first one, a clamped-free beam with $L = 2$ [m] is studied. The first two bending and torsional circular frequencies, ω, are considered. The second analysis examines a simply supported slender beam with a length of 20 [m]. The first four bending modes are taken into account. The results are reported in a non-dimensional form as $\bar{\omega} = \omega\sqrt{\frac{L^4\rho}{Eb^2}}$.

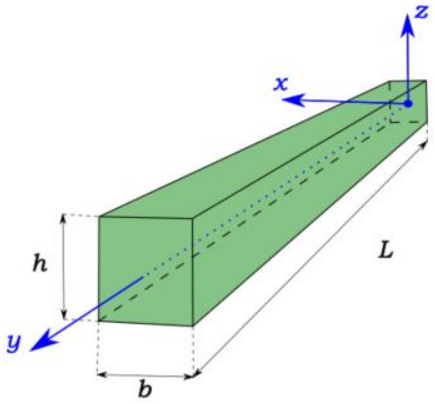

Figure 3: Geometrical properties of a beam.

A convergence analysis for the second torsional frequencies is performed in the clamped-free beam case, see Fig. 4. A fifth-order Taylor expansion is used for the structural theory. The frequencies are normalized as $\omega^* = \frac{\bar{\omega}}{\bar{\omega}_{REF}}$, where $\bar{\omega}_{REF}$ stands for the reference solution from [36].

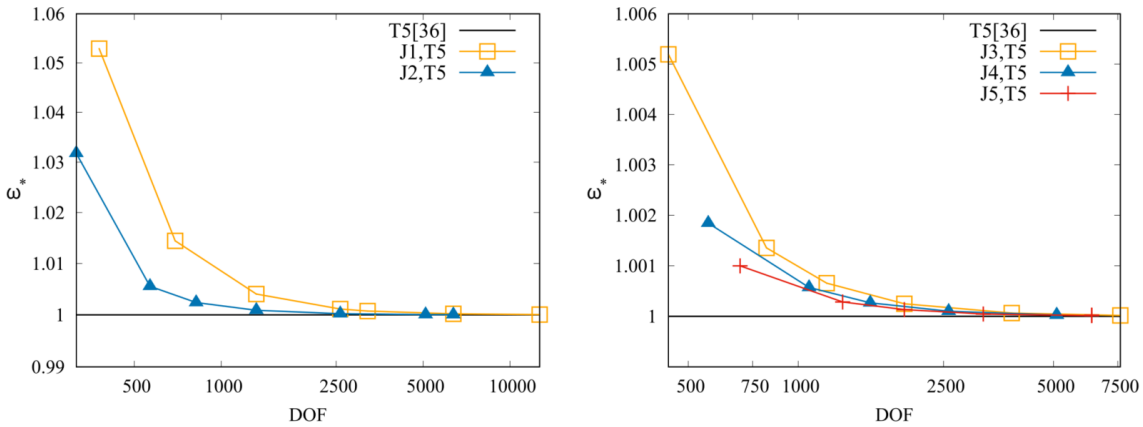

Figure 4: Isotropic clamped free Beam. Convergence of the second torsional non-dimensional circular frequencies with $\boldsymbol{\omega}^* = \frac{\bar{\omega}}{\bar{\omega}_{\mathbf{REF}}}$.

J1,T5 is a very stiff element that reaches convergence when using many DOFs. The convergence rate is very high, starting from the third-order elements. On the other hand, J4 and J5 shape functions are near to the exact solution with few elements.

Table 3 shows the results for several models by using T1 and T5 kinematics. The first column indicates the FE adopted. The central columns show the circular frequencies for different modes.

Table 3: Isotropic Beam. First two bending and torsional non-dimensional circular frequencies.

FEM	I Bending	II Bending	I Torsional	II Torsional	DOF	Nº FEs
			T1[36]			
—	1.008	6.069	9.631	28.893	—	—
			T5[36]			
—	1.013	6.069	8.868	26.603	—	—
			T1			
J1	1.015	6.113	9.632	28.904	459	50
J2	1.007	6.065	9.361	28.894	459	25
J3	1.007	6.065	9.361	28.894	468	17
J4	1.007	6.065	9.361	28.894	477	13
J5	1.007	6.065	9.361	28.894	459	10
			T5			
J1	1.022	6.128	8.871	26.623	3213	50
J2	1.014	6.075	8.869	26.607	3213	25
J3	1.013	6.072	8.869	26.605	3276	17
J4	1.013	6.071	8.868	26.605	3336	13
J5	1.013	6.070	8.868	26.604	3213	10

The following considerations can be made at the end of the analysis:

(a) J1 cannot accurately evaluate the second bending and torsional circular frequencies.

(b) When J2 is adopted, the analysis improves.

(c) From the third-order Jacobi elements, results are near to the reference solution.

(d) T1 from the references are similar to the T1 with the present higher order shape functions. The same can be said for T5.

Figure 5 illustrates the convergence analysis by using T2 for the simply supported slender beam. The fourth bending non-dimensional circular frequencies are considered.

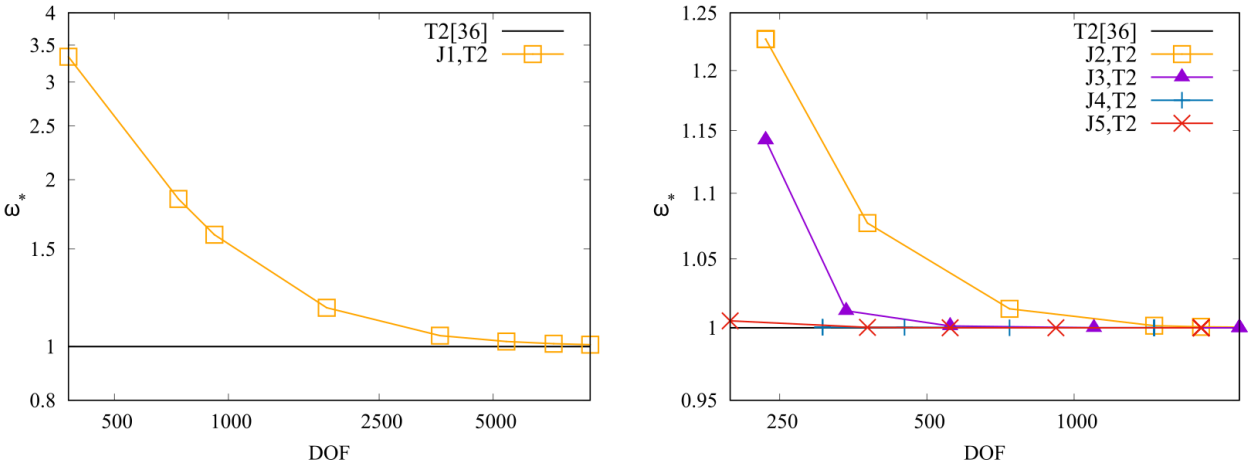

Figure 5: Isotropic simply supported free Beam. Convergence of the fourth bending non-dimensional circular frequencies with $\omega^* = \frac{\bar{\omega}}{\bar{\omega}_{REF}}$.

Furthermore, Table 4 shows the results by using T2 for the simply supported slender beam. In this table, the first four bending frequencies are considered.

Table 4: Isotropic simply supported Beam. First four bending non-dimensional circular frequencies.

FEM	I Bending	II Bending	III Bending	IV Bending	DOF	Nº FEs
			T2[36]			
—	2.849	11.390	25.607	45.478	—	—
			T2			
J1	4.509	18.048	28.184	72.375	918	50
J2	2.850	11.409	25.709	45.796	918	25
J3	2.849	11.390	25.609	45.483	936	17
J4	2.849	11.390	25.608	45.478	954	13
J5	2.849	11.390	25.608	45.478	918	10

Some final remarks can be drawn for this analysis:
(a) Results for the J1 models do not match the reference solutions.
(b) When J2 is adopted, the analysis improves. However, the results inaccurate if the IV Bending mode is considered.
(c) From the third-order Jacobi elements, results are near to the reference solution.

5.2 Isotropic plate

As a second benchmark, a simply supported plate is considered. The geometric characteristics are described in Fig. 6, with $b/h = 2,\ldots,1000$ and $b/a = 1$. The material properties are $E = 73$ [GPa], $\nu = 0.34$, while the material density, $\rho = 2800$ [kg/m^3]. Present results are compared with closed form solutions, denoted as Exact. See [37] for more information. The first fundamental circular frequency, ω, is considered. The results are reported in a non-dimensional form as $\bar{\omega} = \omega\sqrt{\frac{b^4\rho}{Eh^2}}$.

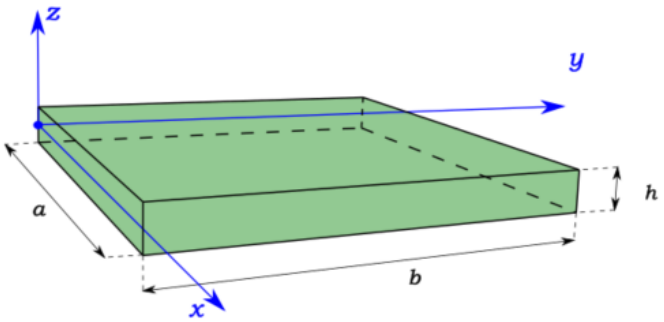

Figure 6: Geometric properties of a simply supported plate.

A convergence analysis is done for a thin plate with b/h = 1000, see Fig. 7. Concerning the structural theory, a fourth-order Taylor expansion is adopted. The frequencies are normalized as $\omega^* = \frac{\bar{\omega}}{\bar{\omega}_{REF}}$, where $\bar{\omega}_{REF}$ indicates the results from the closed form solution.

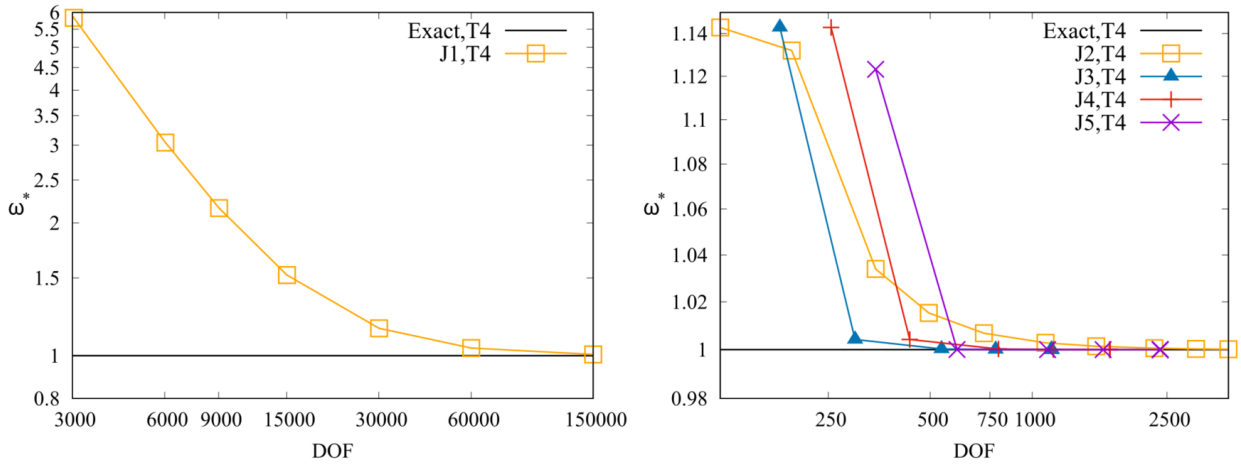

Figure 7: Convergence of the first fundamental non dimensional circular frequency for a thin plate (L/h = 1000) with $\omega^* = \frac{\bar{\omega}}{\bar{\omega}_{REF}}$.

J1,T4 is a very stiff element that reaches convergence when using a great number of DOFs. Starting from the third-order elements, the convergence rate is very high. J4 and J5 shape functions are near the exact solution with a limited number of elements.

Table 4 shows the results for several models by using TPT and T4 kinematics. The relation between the first fundamental non-dimensional circular frequency and length-to-thickness ratios is illustrated. The first column indicates the FE adopted. The central columns show the circular frequencies for several length-to-thickness ratios. Figure 8 illustrates the shear locking issues for the lower order shape functions. The DOFs are the same as in the Table 5.

Table 5: Isotropic plate. First fundamental non-dimensional circular frequency.

FEM \ b/h	2	4	10	100	1000	DOF	Nº FEs
—	2.7586	2.9546	3.0172	3.0295	3.0296	—	—
—	2.2407	2.7429	2.9762	3.0290	3.0295	—	—
J1	3.2917	6.6592	15.531	152.97	15297	444	36
J2	2.7619	2.9596	3.0233	3.0358	3.0360	438	14
J3	2.7586	2.9544	3.0172	3.0295	3.0296	456	9
J4	2.7586	2.9544	3.0172	3.0295	3.0296	462	6
J5	2.7586	2.9544	3.0172	3.0295	3.0296	444	4
J1	2.2433	2.7505	3.0162	5.7081	48.469	1110	36
J2	2.2408	2.7430	2.9764	3.0349	3.0382	1095	14
J3	2.2407	2.7429	2.9762	3.0291	3.0296	1140	9
J4	2.2407	2.7429	2.9762	3.0290	3.0296	1155	6
J5	2.2407	2.7428	2.9761	3.0290	3.0296	1110	4

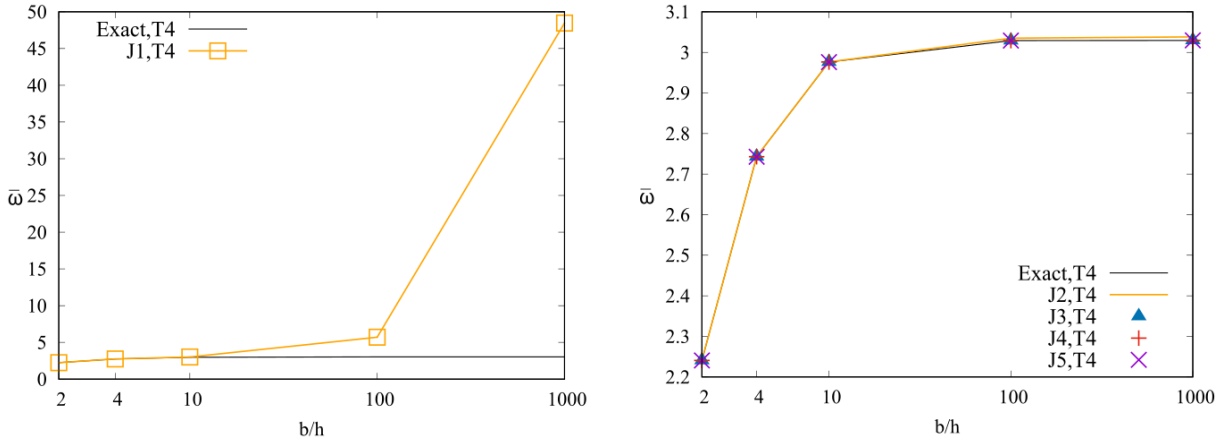

Figure 8: Isotropic plate. Shear locking issues.

The analysis of the plate highlights the followings:
(a) The models with J1 are progressively far from the reference solution when the length-to-thickness ratio increases. Locking problems also affect J2, but with less intensity.
(b) J3, J4 and J5 can approach the reference solution for each length-to-thickness ratio, showing that they are locking-free.
(c) TPT from the references are like the TPT with the present higher order shape functions. The same can be said for T4.

5.3 Isotropic shell

Finally, a simply supported cylindrical shell is taken into account. Figure 9 illustrates the geometric characteristics, with $R_\beta/b = \pi/3$, $R_\beta/h = 2, \ldots, 1000$ and $b/a = 1$. A curvilinear reference system is adopted, and the shell curvature is on the β axis. The material properties are the same as the previous isotropic plate. The study case is taken from [38]. Present results are compared with closed form solutions. The first fundamental circular frequency, ω, is considered. The results are reported in a non-dimensional form as $\bar{\omega} = \omega\sqrt{\frac{R_\beta^4 \rho}{Eh^2}}$.

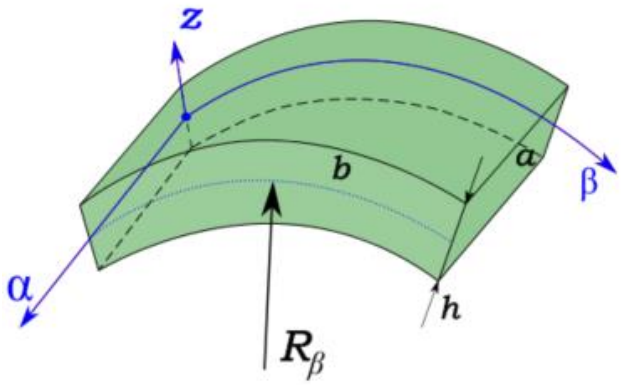

Figure 9: Geometric properties of a simply supported shell.

A convergence analysis is performed for a thin shell with R_β/h = 1000, see Fig. 10. A fourth-order Taylor expansion is chosen as the structural theory. The frequencies are normalized as $\omega^* = \frac{\bar{\omega}}{\bar{\omega}_{REF}}$. $\bar{\omega}_{REF}$ stands for the closed form solution from [38].

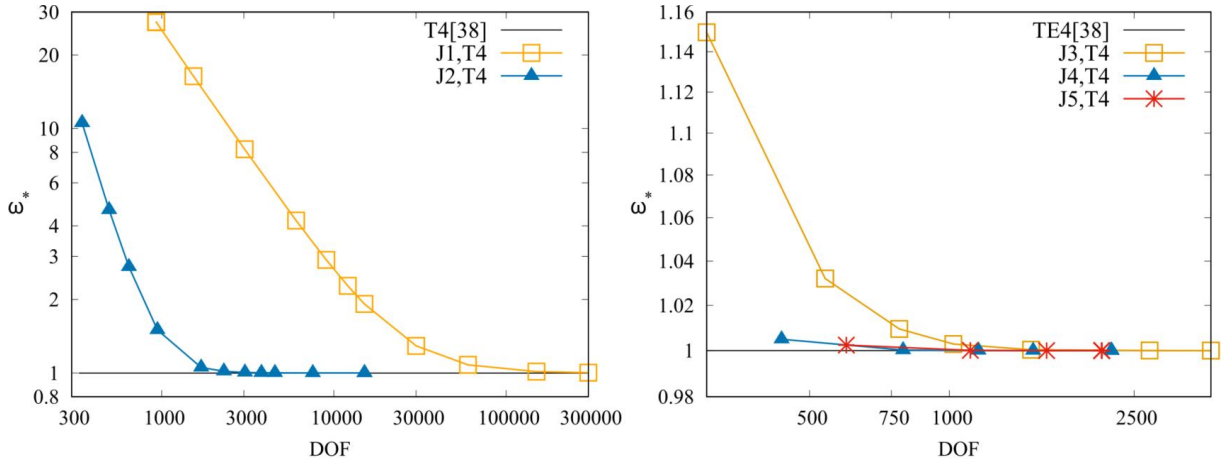

Figure 10: Convergence of the first fundamental non-dimensional circular frequency for the thin shell (R_β/h = 1000) with $\omega^* = \frac{\bar{\omega}}{\bar{\omega}_{REF}}$.

J1, T4 is a very stiff element that reaches convergence when using a significant number of DOFs. In the shell case, also the third-order elements show a low convergence rate. J4 and J5 shape functions are near the exact solution with few elements.

Table 6 shows the results for several models using TST and T4 kinematics. The relation between the first fundamental non-dimensional circular frequency and radius-to-thickness ratios is illustrated. The first column indicates the FE adopted. The central columns show the circular frequencies for different radius-to-thickness ratios. Finally, Figure 11 shows how the lower order shape functions are affected by the shear locking issues for high radius-to-thickness ratios. The DOFs are the same as in the Table 6.

Table 6: Isotropic cylindrical shell. First fundamental non-dimensional circular frequency.

FEM \ R_β/h	2	4	10	100	1000	DOF	Nº FEs
				TST[38]			
—	2.2574	2.3087	2.3261	2.3296	2.3296	—	—
				T4[38]			
—	1.8239	2.1537	2.2976	2.3293	2.3296	—	—
				TST			
J1	2.8648	4.3053	9.4616	91.733	916.98	660	54
J2	2.2578	2.3103	2.3284	2.3334	2.4269	678	22
J3	2.2569	2.3085	2.3261	2.3296	2.3302	600	14
J4	2.2569	2.3085	2.3261	2.3296	2.3297	606	8
J5	2.2568	2.3085	2.3261	2.3296	2.3297	648	6
				T4			
J1	1.8256	2.1587	2.3251	4.2269	35.345	1650	54
J2	1.8239	2.1537	2.2977	2.3323	2.4562	1695	22
J3	1.8239	2.1537	2.2977	2.3294	2.3305	1500	14
J4	1.8239	2.1537	2.2977	2.3293	2.3297	1515	8
J5	1.8238	2.1537	2.2975	2.3293	2.3297	1620	6

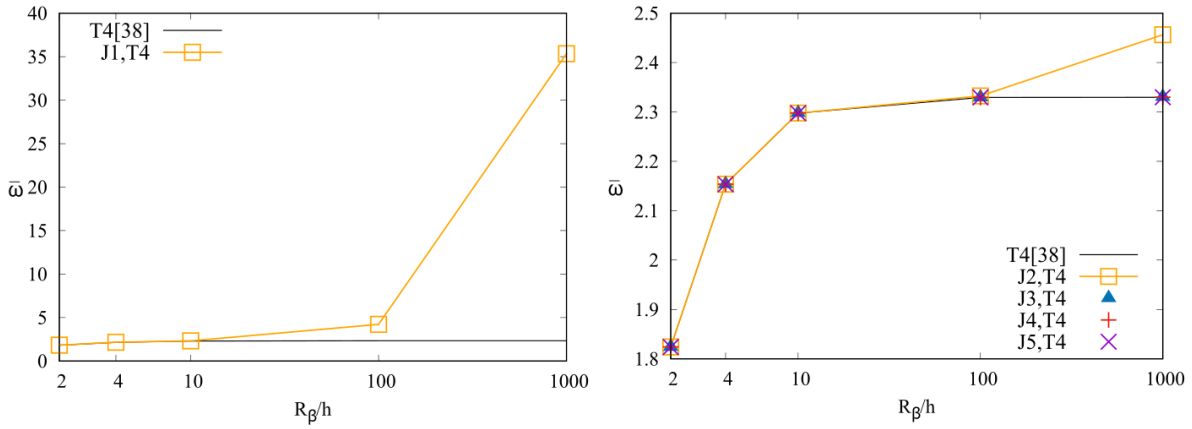

Figure 11: Isotropic cylindrical shell. Shear locking issues.

The following considerations can be drawn:
(a) J1 models are progressively far from the reference solution when the length-to-thickness ratio increases. Locking problems also affect J2 for thin cases.
(b) Shear locking is present also for J3, especially for R_β/h = 1000.
(c) J4 and J5 match the reference solutions for each radius-to-thickness ratio, demonstrating the capability to mitigate the locking issues.
(d) TST from the references match the TST with the present higher order shape functions. It is also true for T4 cases.

6 Conclusions

The present work presented the free vibration analysis of beams, plates, and shells by means of Jacobi-like finite elements based on the CUF. Various geometries and boundary conditions are considered and one-dimensional (1D) beam, two-dimensional (2D) plate and shell models are employed. Three case studies were considered. Finally, results are compared with reference and analytical solutions.

(a) Regarding the circular frequencies, the proposed FEs are demonstrated to be reliable with respect to the reference solutions.
(b) Concerning the beam, bending and torsional modes are similar to the reference solutions when shape functions with higher-polynomial orders are used.
(c) For the plate and shell, it is demonstrated that shear locking is progressively counteracted by augmenting the polynomial order of the shape functions.
(d) The same conclusions drawn by Carrera et al. [13] are shown, i.e., parameters γ and θ are not influential for the calculations.

References

[1] R.H. MacNeal. Perspective on finite elements for shell analysis. Finite Elements in Analysis and Design, 30:175–176, 1998.

[2] L. Euler. Methodus inveniendi lineas curvas maximi minimive proprietate gaudentes sive solutio problematis isoperimetrici latissimo sensu accepti, volume 1. Springer Science & Business Media, Berlin, Germany, 1952.

[3] S.P. Timoshenko. On the transverse vibrations of bars of uniform cross section. Philosophical Magazine, 43:125–131, 1922.

[4] E. Carrera, A. Pagani, M. Petrolo, and E. Zappino. Recent developments on refine theories for beams with applications. Mechanical Engineering Reviews, 2(2):14–00298–14–00298, 2015.

[5] K.J. Bathe. Finite Element Procedure. Prentice hall, Upper Saddle River, New Jersey, USA, 1996.

[6] E. Carrera, M. Cinefra, M. Petrolo, and E. Zappino. Finite element analysis of structures through unified formulation. John Wiley & Sons, 2014.

[7] G. Kirchhoff. ¨Uber das Gleichgewicht und die Bewegung einer elastischen Scheibe. Journal für die reine und angewandte Mathematik, 40:51–88, 1850.

[8] E. Reissner. The effect of transverse shear deformation on the bending of elastic plates. Journal of Applied Mechanics, 12:69–77, 1945.

[9] R.D. Mindlin. Influence of rotary inertia and shear on flexural motions of isotropic, elastic plates. Journal of Applied Mechanics-transactions of the ASME, 18:31–38, 1951.

[10] J.H. Argyris. Matrix displacement analysis of plates and shells, prolegomena to a general theory, Part I. Ingeniur-Archiv, 35:102–142, 1966.

[11] K.J. Bathe and L.W. Ho. Some results in the analysis of thin shell structures. In W. Wunderlich, E. Stein, and K.J. Bathe, editors, Nonlinear Finite Element Analysis in Structural Mechanics, pages 122–150, Berlin, Heidelberg, 1981. Springer Berlin Heidelberg.

[12] E. Carrera. C_0 Reissner–Mindlin multilayered plate elements including zig-zag and interlaminar stress continuity. International Journal for Numerical Methods in Engineering, 39(11):1797–1820, 1996.

[13] E. Carrera, R. Augello, A. Pagani, and D. Scano. Refined multilayered beam, plate and shell elements based on Jacobi polynomials. Composite Structures, 304:116275, 2023.

[14] M. Abramowitz and I.A. Stegun. Handbook of Mathematical Functions with Formulas, Graphs, and Mathematical Tables. Dover Publications, 1964.

[15] F. Fuentes, B. Keith, L. Demkowicz, and S. Nagaraj. Orientation embedded high order shape functions for the exact sequence elements of all shapes. Computers & Mathematics with Applications, 70(4):353–458, 2015.

[16] B. Szabo, A. Duester, and E. Rank. The p-Version of the Finite Element Method, Chapter 5. John Wiley & Sons, 2011.

[17] E. Zappino, G. Li, A. Pagani, E. Carrera, and A.G. de Miguel. Use of higher-order Legendre polynomials for multilayered plate elements with node-dependent kinematics. Composite Structures, 202:222–232, 2018. Special issue dedicated to Ian Marshall.

[18] M. Cinefra. Free-vibration analysis of laminated shells via refined MITC9 elements, Mechanics of Advanced Materials and Structures, 23:9, 937-947, 2016.

[19] A. Pagani, A.G. de Miguel, M. Petrolo, and E. Carrera. Analysis of laminated beams via unified formulation and Legendre polynomial expansions. Composite Structures, 156:78– 92, 2016. 70th Anniversary of Professor J. N. Reddy.

[20] M. Cinefra and S. Valvano. A variable kinematic doubly-curved MITC9 shell element for the analysis of laminated composites, Mechanics of Advanced Materials and Structures, 23:11, 1312-1325, 2016.

[21] A. Pagani, E. Carrera, and A.J.M. Ferreira Higher-order theories and radial basis functions applied to free vibration analysis of thin-walled beams, Mechanics of Advanced Materials and Structures, 23:9, 1080-1091, 2016.

[22] E. Carrera. Developments, ideas, and evaluations based upon Reissner's Mixed Variational Theorem in the modeling of multilayered plates and shells. Appl. Mech. Rev., 54(4):301–329, 2001.

[23] R.K. Kapania and S. Raciti. Recent advances in analysis of laminated beams and plates, part II: Vibrations and wave propagation. AIAA Journal, 27(7):935–946, 1989.

[24] E. Carrera, M. Filippi, and E. Zappino. Free vibration of laminated beam by polynomial, trigonometric, exponential and zig-zag theories. Journal of Composite Materials, 2013.

[25] Y. Yan, E. Carrera, and A. Pagani. Free vibration analysis of curved metallic and composite beam structures using a novel variable-kinematic DQ method, Mechanics of Advanced Materials and Structures, 29:25, 3743-3762, 2022.

[26] M. Cinefra and M. Soave. Accurate Vibration Analysis of Multilayered Plates Made of Functionally Graded Materials, Mechanics of Advanced Materials and Structures, 18:1, 3-13, 2011.

[27] K.P. Soldatos. Influence of thickness shear deformation on free vibrations of rectangular plates, cylindrical panels and cylinders of antisymmetric angle-ply construction. Journal of Sound and Vibration, Vol. 119, pp.111–137, 1987.

[28] L.H. Donnell. Stability of thin-walled tubes under torsion. NACA Report 479, 1933.

[29] L. Sanders. Nonlinear theories for thin shells. Quarterly of Applied Mathematics, Vol. 21, pp.21–36, 1963.

[30] W. Flügge. Statik und Dynamik der Schalen, Springer-Verlag, Berlin, 1934.

[31] C.T. Loy, K.Y Lam, and J.N. Reddy. Vibration of functionally graded cylindrical shells, International Journal of Mechanical Science, Vol. 41, No. 3, p.30924, 1999.

[32] H. Matsunaga. Vibration and buckling of cross-ply laminated composite circular cylindrical shells according to a global higher-order theory, International Journal of Mechanical Science, Vol. 49, No. 9, p.106075, 2007.

[33] E. Carrera. The effects of shear deformation and curvature on buckling and vibrations of cross-ply laminated composite shells. Journal of Sound and Vibrations, Vol. 150, No. 3, pp.405–433, 1991.

[34] E. Zappino, T. Cavallo, and E. Carrera. Free vibration analysis of reinforced thin-walled plates and shells through various finite element models, Mechanics of Advanced Materials and Structures, 23:9, 1005-1018, 2016.

[35] E. Carrera. Theories and finite elements for multilayered plates and shells: a unified compact formulation with numerical assessment and benchmarking. Archives of Computational Methods in Engineering, 10(3):215–296, 2003.

[36] A. Pagani, M. Boscolo, J.R. Banerjee, and E. Carrera. Exact dynamic stiffness elements based on one-dimensional higher-order theories for free vibration analysis of solid and thin-walled structures. Journal of Sound and Vibration, 332(23):6104–6127, 2013.

[37] E. Carrera. Developments, ideas, and evaluations based upon Reissner's Mixed Variational Theorem in the modeling of multilayered plates and shells. Appl. Mech. Rev., 54(4):301–329, 2001.

[38] E. Carrera, C. Campisi, M. Cinefra, and M. Soave. Evaluation of various theories of the thickness and curvature approximations for free vibrational analysis of cylindrical and spherical shells. International Journal of Vehicle Noise and Vibration, 7(1):16–36, 2011.